Cellular Sequestration of Cadmium in the Hyperaccumulator Plant Species *Sedum alfredii*[1][C][W]

Shengke Tian, Lingli Lu, John Labavitch, Xiaoe Yang*, Zhenli He, Hening Hu, Ritimukta Sarangi, Matt Newville, Joel Commisso, and Patrick Brown

Ministry of Education Key Laboratory of Environment Remediation and Ecological Health, College of Environmental and Resource Science, Zhejiang University, Hangzhou 310058, China (S.T., L.L., X.Y.); Department of Plant Sciences, University of California, Davis, California 95616 (S.T., L.L., J.L., H.H., J.C., P.B.); Indian River Research and Education Center, Institute of Food and Agricultural Science, University of Florida, Fort Pierce, Florida 34945 (Z.H.); Stanford Synchrotron Radiation Lightsource, Stanford Linear Accelerator Center National Accelerator Laboratory, Menlo Park, California 94025 (R.S.); and GSECARS Advanced Photon Source, Argonne National Laboratory, Argonne, Illinois 60439 (M.N.)

Spatial imaging of cadmium (Cd) in the hyperaccumulator *Sedum alfredii* was investigated in vivo by laser ablation inductively coupled plasma mass spectrometry and x-ray microfluorescence imaging. Preferential Cd accumulation in the pith and cortex was observed in stems of the Cd hyperaccumulating ecotype (HE), whereas Cd was restricted to the vascular bundles in its contrasting nonhyperaccumulating ecotype. Cd concentrations of up to 15,000 μg g^{-1} were measured in the pith cells, which was many fold higher than the concentrations in the stem epidermis and vascular bundles in the HE plants. In the leaves of the HE, Cd was mainly localized to the mesophyll and vascular cells rather than the epidermis. The distribution pattern of Cd in both stems and leaves of the HE was very similar to calcium but not zinc, irrespective of Cd exposure levels. Extended x-ray absorption fine structure spectroscopy analysis showed that Cd in the stems and leaves of the HE was mainly associated with oxygen ligands, and a larger proportion (about 70% in leaves and 47% in stems) of Cd was bound with malic acid, which was the major organic acid in the shoots of the plants. These results indicate that a majority of Cd in HE accumulates in the parenchyma cells, especially in stems, and is likely associated with calcium pathways and bound with organic acid (malate), which is indicative of a critical role of vacuolar sequestration of Cd in the HE *S. alfredii*.

Metal hyperaccumulation and the associated hypertolerance in plants is a naturally selected, extreme, and complex physiological trait found in a small number of species (Kramer, 2010). An understanding of the processes involved in metal accumulation in the hyperaccumulators is helpful to understand natural genetic variations in plant development, physiology, and adaptation under harsh environmental conditions (Alonso-Blanco et al., 2009; Kramer, 2010) and to facilitate the optimization of plant-based strategies for phytoremediation/phytoextraction (Chaney et al., 2007) as well as biofortification in the case of micronutrients (Zhao and McGrath, 2009). A better understanding of the highly effective detoxification mechanism that allows the survival of hyperaccumulators at uniquely high internal metal concentrations may also facilitate the discovery of remedies for the debilitating effects of metal pollution on human health (Kramer, 2010).

In the last decade, significant progress has been made in the understanding of the physiology and molecular mechanism of heavy metal hyperaccumulation (Pence et al., 2000; Hanikenne et al., 2008). Still, minimal information is available on cadmium (Cd) accumulation in plants, as hyperaccumulation of Cd is a very rare phenomenon due to its nonessential nature and high phytotoxicity to plants. Cd hyperaccumulation, defined as the accumulation and tolerance of up to 100 μg Cd g^{-1} in shoots by plants (Baker et al., 2000), is present only in some populations of *Thlaspi caerulescens*, *Arabidopsis halleri*, and *Thlaspi praecox*, all belonging to the Brassicaceae family, and *Sedum alfredii* (Crassulaceae; Verbruggen et al., 2009; Kramer, 2010). *S. alfredii* is a zinc (Zn)/Cd cohyperaccumulator and lead (Pb) accumulator, which was also of high tolerance to copper toxicity, discovered in a Pb/Zn-rich region of China (Yang et al., 2002, 2004; Tian et al., 2010). The plants of the hyperaccumulating ecotype (HE) of *S. alfredii* collected from the Pb/Zn mined site are much more

[1] This work was supported by the National Natural Science Foundation of China (grant nos. 30630046 and 31000935), the Ministry of Education of China (grant no. 310003), the Ministry of Environmental Protection of China (grant no. 2011467057), and the China Postdoctoral Science Foundation (grant no. 201104731).

* Corresponding author; e-mail phbrown@ucdavis.edu.

The author responsible for distribution of materials integral to the findings presented in this article in accordance with the policy described in the Instructions for Authors (www.plantphysiol.org) is: Xiaoe Yang (xyang571@yahoo.com).

[C] Some figures in this article are displayed in color online but in black and white in the print edition.

[W] The online version of this article contains Web-only data.

www.plantphysiol.org/cgi/doi/10.1104/pp.111.183947

tolerant to Cd stress as compared with the nonhyperaccumulating ecotype (NHE; Supplemental Fig. S1A). *S. alfredii* has attracted significant attention in recent years both for its unique characteristics and potential utilization in phytoremediation, especially in China (Deng et al., 2007; Wu et al., 2007; Sun et al., 2009). *S. alfredii*, however, is much less studied as compared with the other two Zn/Cd hyperaccumulators, *T. caerulescens* and *A. halleri*.

As a nonessential element, Cd is preferentially partitioned in roots of normal plants but translocated to the aerial parts of the hyperaccumulators (Conn and Gilliham, 2010). Hyperaccumulator species appear to protect roots from metal toxicity partially through efficient shuttling of metals to the shoot (Kramer, 2010), possibly as a result of efficient root uptake, reduced root cell sequestration, and enhanced xylem loading (Verbruggen et al., 2009). Our previous work on the hyperaccumulator *S. alfredii* suggested that more than 60% of the total Cd taken up by the plants was partitioned to the shoots after 3 d of exposure to Cd solutions (Lu et al., 2008). Cd concentrations in leaves and stems of the HE *S. alfredii* of up to 4,000 μg g^{-1} after 100 μM Cd exposure for 30 d have been observed, whereas Cd levels in shoots of the NHE were much lower (Supplemental Fig. S1B). This enhanced root-to-shoot translocation and hyperaccumulation of Cd in the HE suggests the presence of a high-capacity metal storage mechanism within the shoots of the HE *S. alfredii*.

To minimize the damage from exposure to excess metal ions, hyperaccumulating species utilize mechanisms including compartmentalization and ligand chelation. Previous studies have suggested that heavy metals mostly accumulate in shoot epidermal and surface structures in the hyperaccumulators, especially in vacuoles (Küpper et al., 2001; Robinson et al., 2003), whereas some research has indicated a dominant role of mesophyll cells in the compartmental detoxification of abundant heavy metals (Küpper et al., 2000; Zhao et al., 2000; Ma et al., 2005). Our previous studies suggested that Pb was largely retained in the cell walls during transportation in plants of *S. alfredii* (Tian et al., 2010), while epidermal layers serve as important storage sites for accumulated Zn in this plant species (Tian et al., 2009). Transmission electron microscopy has been used to investigate the subcellular distribution of Cd in leaf tissues of the hyperaccumulator *S. alfredii* (Zhang et al., 2010); however, this method is subject to artifacts, as Cd could redistribute during the complex sample preparation.

X-ray microfluorescence (μ-XRF) has been widely used in research on elemental distribution in plant tissues and has proved to be a promising tool to study the in vivo localization of metals in plants (Punshon et al., 2009). In this study, the in vivo characteristics of Cd distribution in stems of the Cd hyperaccumulating ecotype (HE) of *S. alfredii* was investigated by using μ-XRF, in comparison with its contrasting non-

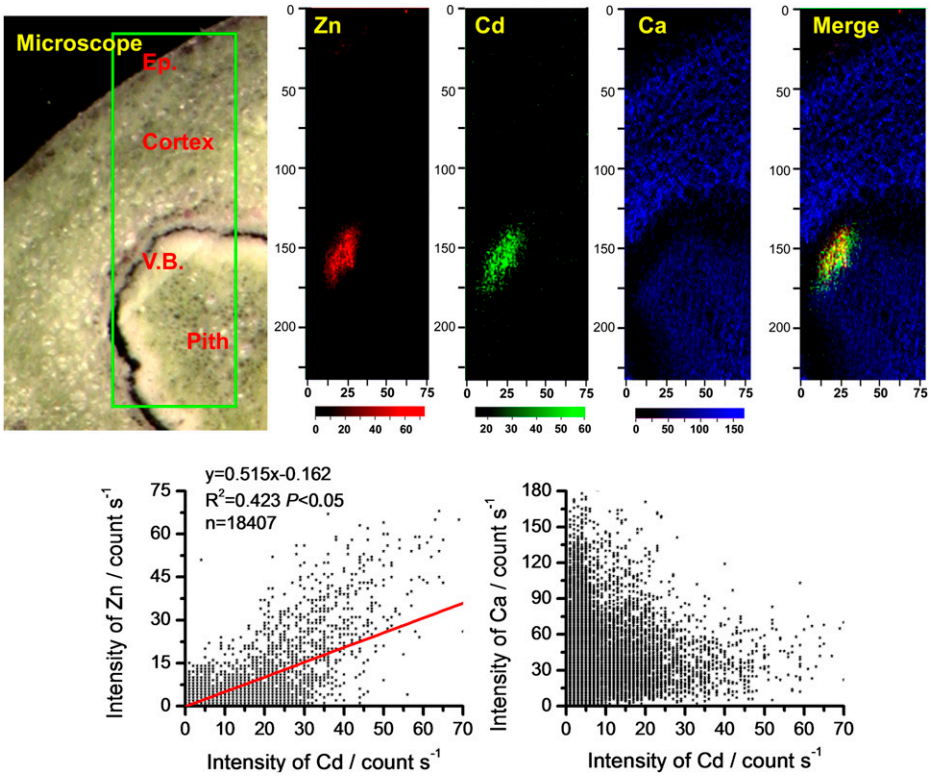

Figure 1. μ-XRF elemental maps for Zn (red), Cd (green), and Ca (blue) of stem cross sections from NHE *S. alfredii* treated with 10 μM Cd. The number of fluorescence yield counts was normalized by I_0 and the dwell time. Pixel brightness is displayed in RGB, with the brightest spots corresponding to the highest element fluorescence. Ep., Epidermis; V.B., vascular bundles. Correlations between XRF intensities of Cd versus Zn and Cd versus Ca were measured according to the XRF data.

hyperaccumulating ecotype (NHE). This technique, however, can only provide semiquantitative information. Laser ablation inductively coupled plasma mass spectrometry (LA-ICP-MS) is a powerful analytical technique for direct elemental mapping of abiotic and biotic samples (Hu et al., 2008) and was used here as a supplemental method of elemental mapping of the HE *S. alfredii* plants under Cd exposure. Additionally, the speciation of Cd within HE *S. alfredii* plants was investigated by extended x-ray absorption fine structure (EXAFS). This is an element-specific method for analyzing the in vivo ligand environment of metals in plants (Küpper et al., 2004). While most previous analyses of the chemical form of Cd have been performed using freeze-dried ground samples with nonfocused x-rays, here, EXAFS was used to investigate the ligand environment of Cd in frozen hydrated tissues of the HE *S. alfredii* under very low temperature.

RESULTS

Comparative Study of Cd Distribution in Stems of NHE and HE by μ-XRF

The distribution patterns of Zn (red color), Cd (green color), and calcium (Ca; blue color) in stem cross sections from NHE and HE *S. alfredii* plants treated with Cd were primarily investigated by μ-XRF (Figs. 1–3). Pixel brightness is displayed in RGB, with the brightest spots corresponding to the highest element fluorescence. The elemental maps of potassium (K), manganese (Mn), iron (Fe), magnesium (Mg), phosphorus (P), and sulfur (S; data not shown) were similar to those reported by Tian et al. (2009, 2010), and there was no significant relationship of these elements with Cd. As shown in Figures 1 and 2, the distribution patterns of Cd were very different between the two contrasting ecotypes of *S. alfredii*. In the stem cross section of 10 μM Cd-treated NHE plants (Fig. 1), Cd

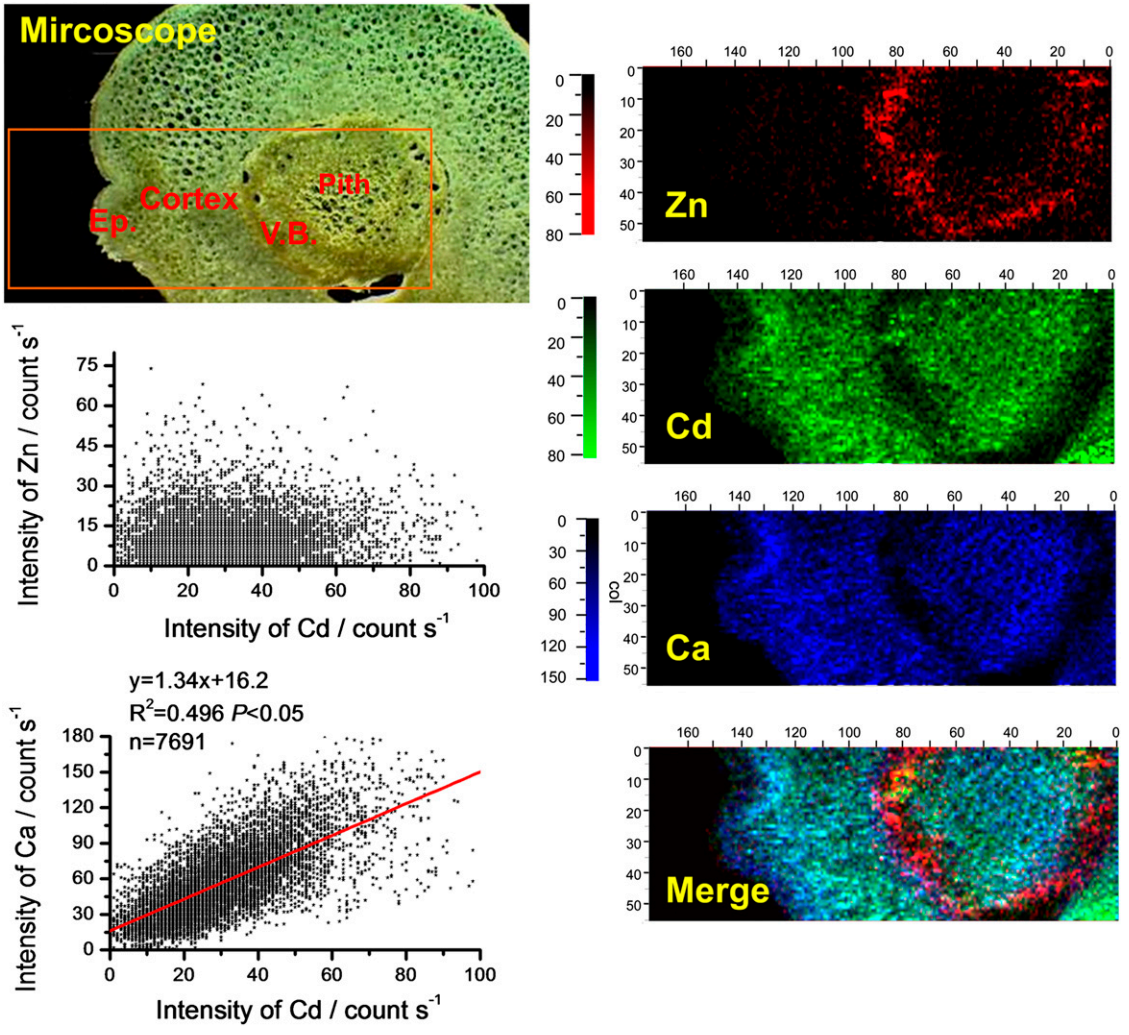

Figure 2. μ-XRF elemental maps for Zn (red), Cd (green), and Ca (blue) of stem cross sections from HE *S. alfredii* treated with 10 μM Cd. The number of fluorescence yield counts was normalized by I_0 and the dwell time. Pixel brightness is displayed in RGB, with the brightest spots corresponding to the highest element fluorescence. Ep., Epidermis; V.B., vascular bundles. Correlations between XRF intensities of Cd versus Zn and Cd versus Ca were derived from the XRF data.

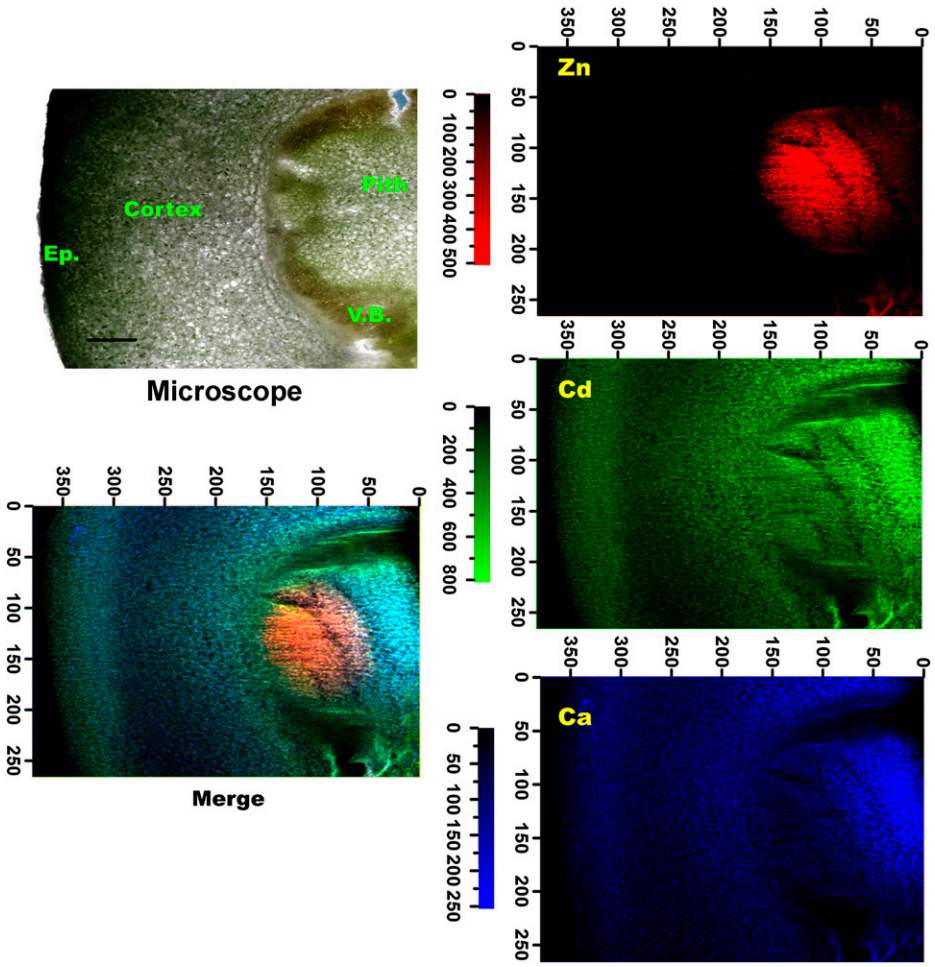

Figure 3. μ-XRF elemental maps for Zn (red), Cd (green), and Ca (blue) of stem cross sections from HE *S. alfredii* treated with 400 μM Cd. The number of fluorescence yield counts was normalized by I_0 and the dwell time. Pixel brightness is displayed in RGB, with the brightest spots corresponding to the highest element fluorescence. Ep., Epidermis; V.B., vascular bundles. Correlations between XRF intensities of Cd versus Zn and Cd versus Ca were measured according to the XRF data.

was distributed mainly in the cells around vascular tissues, in a very similar pattern to that of Zn, whereas Ca was mostly localized to the cortex and pith. In contrast, in the stem cross section of the HE (10 μM Cd), the distribution pattern of Cd was very similar to that of Ca, showing higher concentrations in the parenchyma tissues, while the preferential localization of Zn in the vascular tissues (Fig. 2) was consistent with the results obtained by μ-XRF in our previous work (Tian et al., 2009). Statistical analysis revealed a positive correlation between Cd and Zn in the stems of NHE plants ($P < 0.05$, $r^2 = 0.423$, $n = 18{,}407$; Fig. 1), whereas Cd was positively colocalized with Ca in the stem cross section of the HE *S. alfredii* ($P < 0.05$, $r^2 = 0.496$, $n = 7{,}691$; Fig. 2). Furthermore, increasing Cd treatments to 100 μM (data not shown) or 400 μM (Fig. 3) did not change the distribution patterns of the elements significantly in the stem of the HE plants, and Cd and Ca were consistently localized in similar parenchyma tissues.

Quantitative Analysis of Cd Distribution in HE Stems by LA-ICP-MS

To confirm the results obtained by μ-XRF, in vivo analysis of Cd distribution in both stems and leaves of the HE *S. alfredii* was performed quantitatively by LA-ICP-MS. The stem and leaf samples were collected from 100 μM Cd-treated HE plants and ablated line by line using a focused laser beam. The ion intensity of $^{13}C^+$ was monitored during measurement for internal standardization to compensate for the different amounts of ablated material (Wu et al., 2009). $^{13}C^+$ was evenly distributed in the plant samples (Fig. 4).

The elemental mapping of stem cross sections of the HE *S. alfredii* after 100 μM Cd treatment confirmed that the distribution pattern of Cd was extremely similar to that of Ca, showing higher concentrations in the pith and cortex tissues, both of which consist of parenchyma cells, rather than vascular bundles and epidermis. As shown in Figure 4, Cd concentration in the cortex was up to 15,000 $\mu g\ g^{-1}$, which was dozens of times higher than those measured in the vascular tissues. Very low Cd concentration was observed in the epidermis and vascular bundles. Zinc was preferentially sequestered by cells near vascular bundles and also in the epidermis, and K was distributed mostly in the tissues of vascular bundles and epidermis. An accumulation of P was observed in the vascular tissues, and S was distributed uniformly throughout the whole stem (Fig. 4).

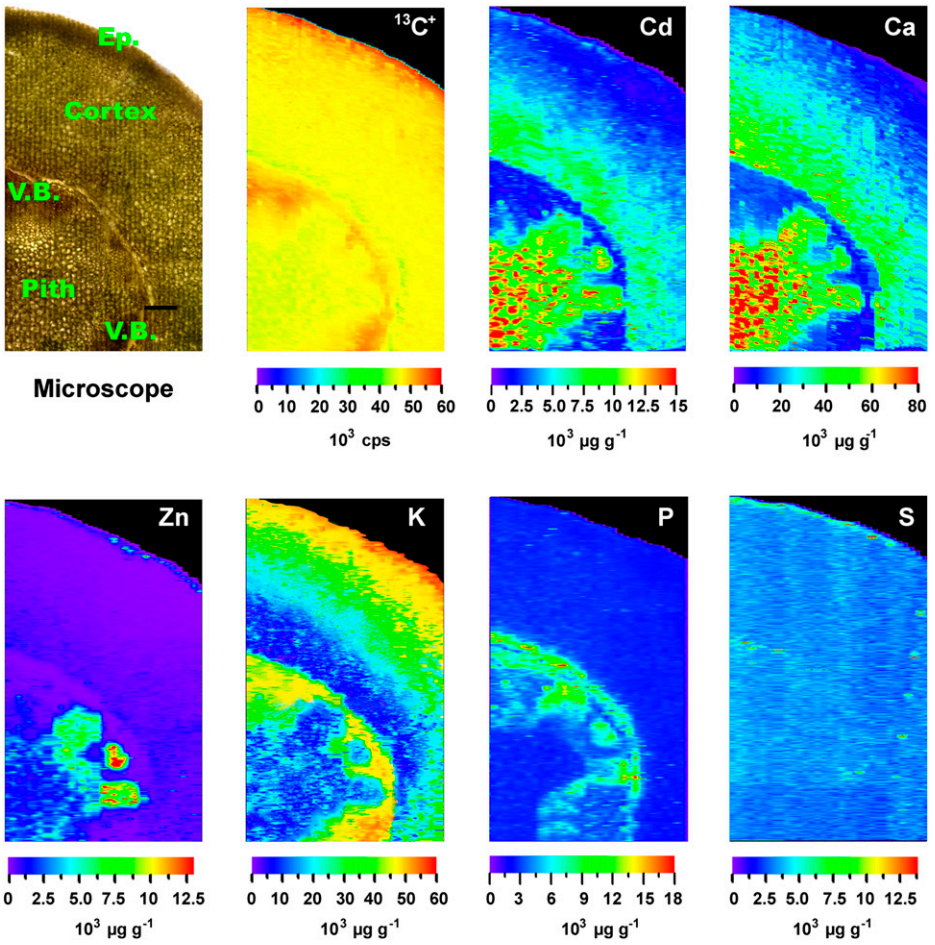

Figure 4. Quantitative images of elements Cd, Ca, Zn, K, P, and S measured by LA-ICP-MS in stem cross sections of the HE *S. alfredii* after 100 μM Cd exposure for 30 d. Ep., Epidermis; V.B., vascular bundles. Bar = 200 μm.

Quantitative Analysis of Cd Distribution in HE Leaves by LA-ICP-MS

Elemental distributions were analyzed by LA-ICP-MS for the whole leaf collected fresh from 100 μM Cd-treated HE *S. alfredii* without any sample preparation. As shown in Figure 5, the distribution patterns of Cd, Ca, Zn, K, P, and S varied depending on the element. Both Cd and Ca were evenly distributed in the whole leaf except for relatively low concentrations in the leaf tips. Zn appeared to be preferentially localized in the epidermis, and the highest ion intensity of K was found in the leaf tips. Higher concentrations of P were observed in the outer tissue layers, while S was localized more evenly except for a low concentration in the tips. No significant correlation of Cd and P or S was observed at the whole leaf level.

Cross sections of leaves from Cd-treated plants were freeze dried and analyzed by LA-ICP-MS to further characterize the distribution patterns of Cd in the leaves of the HE *S. alfredii* at the cellular level (Fig. 6). The ion intensity of $^{13}C^+$ was very similar across the slice except for the main veins and epidermis tissues, due to the difference in the thickness of these tissues and the mesophyll. Cd and Ca were distributed similarly, showing higher concentrations in palisade mesophyll cells and a peak of Cd in the vascular bundles. Phosphorus was evenly distributed in the leaf cross sections of *S. alfredii*, and relatively higher levels of K were located in vascular, epidermal, and spongy cells, while Zn was predominantly concentrated in epidermal cells. P and S were distributed evenly across the cross section of the leaf.

Cd Species in the Tissues of the HE *S. alfredii*

Bulk-EXAFS was employed to investigate the Cd speciation in the powdered fractions of the leaf and stem for the HE *S. alfredii* treated with 100 μM Cd for 30 d, which contained adequate metal concentrations to obtain good signal-to-noise ratios. The low concentrations of Cd in the plant samples of the NHE *S. alfredii* prevented analysis of Cd speciation by this technique.

Figure 7 shows Cd K-edge, K^3-weighted EXAFS spectra of powdered plant samples (young leaves, mature leaves, stems, and roots) of the HE *S. alfredii* compared with model compounds, including Cd-His, Cd-glutathione, Cd-Cys, Cd-malate, Cd-oxalate, Cd-citrate, Cd^{2+} [$Cd(NO_3)_2$], and Cd-cell wall. The results of the EXAFS data following refinement with SixPack for the Cd ligands environment in plant samples of the

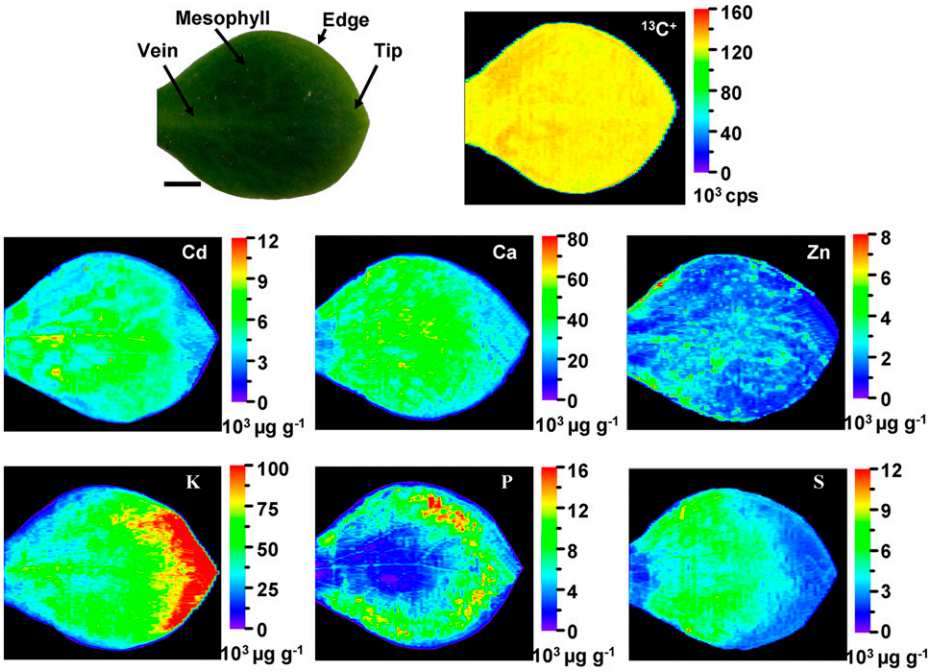

Figure 5. Quantitative images of elements Cd, Ca, Zn, K, P, and S measured by LA-ICP-MS in whole leaves of the HE *S. alfredii* after 100 μM Cd exposure for 30 d. Bar = 4.0 mm.

HE *S. alfredii* are summarized in Table I. The ligand environment in the plant samples differed depending on the plant tissues sampled. Cd in the leaves (both young and mature leaves) and stems was exclusively coordinated with oxygen (O) ligands. However, a first shell coordination of O with the addition of S was detected as the main contribution in the root samples. The spectra were then analyzed using linear combination fitting (Table II). This analysis revealed that the dominant chemical form of Cd in shoots of the HE *S. alfredii* (about 70% in leaves and 47% in stems) was similar to Cd-malate compounds, with the remaining

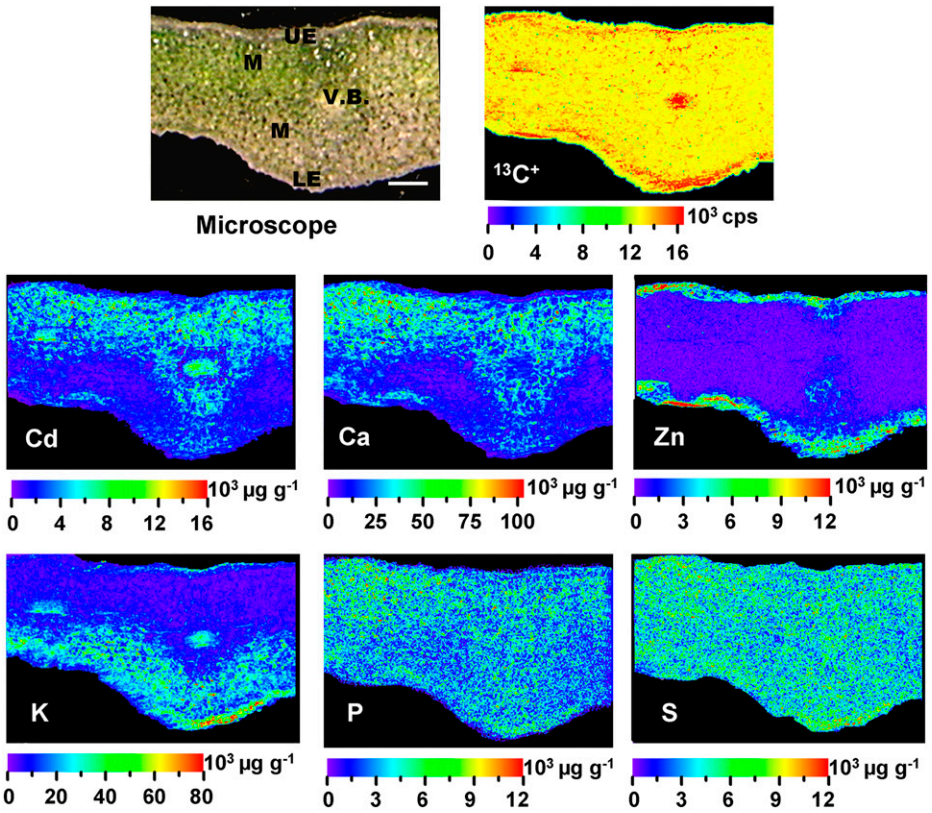

Figure 6. Quantitative images of elements Cd, Ca, Zn, K, P, and S measured by LA-ICP-MS in leaf cross sections of the HE *S. alfredii* after 100 μM Cd exposure for 30 d. LE, Lower epidermis; M, mesophyll; UE, upper epidermis; V.B., vascular bundles. Bar = 200 μm.

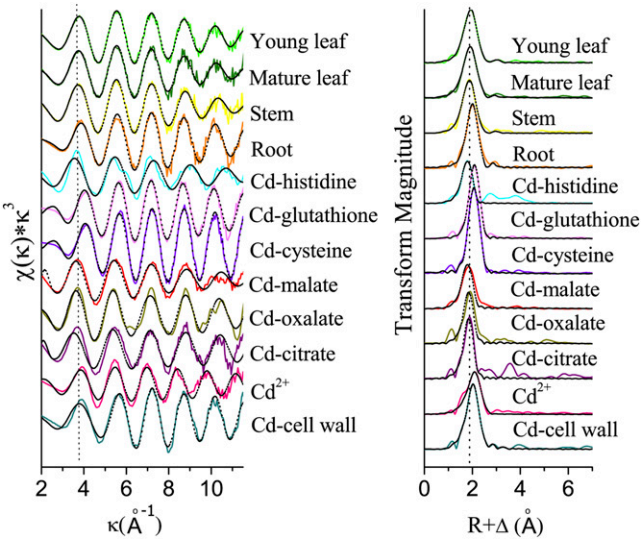

Figure 7. Left, Cd K-edge, K^3-weighted EXAFS spectra for powdered plant samples of the HE *S. alfredii* treated with 100 μM Cd, and model compounds (solid lines) with best linear combination fits (dashed black lines). Right, Stacked radial structure functions (not corrected for phase shift) from Cd K-edge, K^3-weighted EXAFS data. Solid and dashed lines are Fourier transform magnitude and imaginary part, respectively. [See online article for color version of this figure.]

proportion of the metal associated as Cd-citrate and Cd-cell wall. In the roots of the HE *S. alfredii*, however, the percentage of Cd-malate complex is quite low, and a large amount of the metal appeared to be associated with cell wall, citrate, and sulfhydryl groups (GSH).

Organic Acids in Plants of the HE *S. alfredii*

In the stems and leaves of the HE *S. alfredii*, the predominant organic acids were malic acid followed by citric and oxalic acids (Table III). Fumarate, pyruvate, acetic acid, and amber acid were not detected. This is consistent with results previously reported by Yang et al. (2006). Regardless of the treatments, the concentrations of malic acid in the stems and leaves of the HE *S. alfredii* were higher than 35 μmol g^{-1} fresh weight, about 6-fold of that in the roots, whereas the concentrations of both citric acid and oxalic acid in the roots were significantly higher than those in the stems and leaves. When plants were exposed to 100 μM Cd, all three organic acids increased nonsignificantly as compared with the controls.

DISCUSSION

Metal sequestration in less bioactive cells such as epidermis and trichomes is one of the possible mechanisms for heavy metal detoxification in plants (Hall, 2002). Based on in vivo analysis by μ-XRF and LA-ICP-MS, both of which are very effective tools for the determination of metal distribution (Hu et al., 2008; Punshon et al., 2009), preferential Cd accumulation in the parenchyma cells (mesophyll, cortex, and pith) was consistently observed in both leaves and stems of the HE *S. alfredii* under different Cd exposure levels. This differed from its the contrasting ecotype (NHE), in which Cd was restricted within the vascular bundles, suggesting that Cd is easily transported from vascular systems to the storage sites in the HE plants as compared with the NHE plants. The finding that Cd concentrations were highest in parenchyma cells has not been reported in other Cd hyperaccumulators. In the Cd hyperaccumulators *T. caerulescens* and *T. praecox*, Cd was found to be most concentrated within the epidermal cells (Cosio et al., 2005; Ma et al., 2005; Fukuda et al., 2008; Vogel-Mikus et al., 2008a, 2008b), while in *A. halleri*, Cd was most concentrated in certain parts of the trichomes (Küpper et al., 2000; Hokura et al., 2006; Fukuda et al., 2008). Previous studies, however, have also pointed out that because of the tissue mass represented by mesophyll cells, these tissues represent the major storage site of Cd in both *T. caerulescens* and *A. halleri*, with 65% to 70% of total leaf Cd distributed in the mesophyll tissues in the leaves of *T. caerulescens* (Ma et al., 2005), and in *A.*

Table I. *Results of refinement of the EXAFS spectra using SixPack*
SE values represent mathematical SE of the refinement (two σ level).

Cd Level	Sample	Type	N	R	σ^2	R Factor
				Å	10^{-3} Å	
100 μM	Young leaves	O	6.1 ± 0.2	2.27 ± 0.02	0.0012	17
		O	8.2 ± 0.3	2.61 ± 0.03	0.001	
		C	3.4 ± 0.1	3.18 ± 0.02	0.011	
	Mature leaves	O	6.4 ± 0.1	2.23 ± 0.02	0.004	12
		O	5.1 ± 0.2	2.66 ± 0.02	0.005	
		C	2.5 ± 0.3	3.25 ± 0.03	0.0034	
	Stems	O	6.0 ± 0.1	2.21 ± 0.01	0.003	21
		O	5.8 ± 0.2	2.62 ± 0.02	0.002	
		C	3.4 ± 0.1	3.18 ± 0.01	0.013	
	Roots	O	6.1 ± 0.1	2.31 ± 0.01	0.009	20
		S	3.6 ± 0.2	2.51 ± 0.02	0.004	
		C	2.1 ± 0.1	3.13 ± 0.03	0.008	

Table II. *Proportion (in % mole fraction) of Cd species in S. alfredii by linear combination fitting*
SE values represent mathematical SE of the refinement (two σ level).

Sample	Cd Species					
	Cd-Malate	Cd-Citrate	Cd-GSH	Cd-Cell Wall	Sum	Residual
			%			
Young leaves	69.3 ± 3.5	15.4 ± 2.3	–	20.5 ± 1.5	105.2	15.5
Mature leaves	72.3 ± 4.2	9.2 ± 1.2	–	17.6 ± 2.1	99.1	24.4
Stems	47.2 ± 2.5	21.7 ± 1.7	–	31.6 ± 2.3	100.5	25.9
Roots	16.7 ± 3.5	24.9 ± 2.4	24.2 ± 2.3	38.9 ± 3.7	104.7	18.4

halleri, epidermal cells other than trichomes contained less Cd than mesophyll cells (Küpper et al., 2000). These results are consistent with our findings here, suggesting that Cd sequestration in the parenchyma (mesophyll) cells is an important strategy for Cd hyperaccumulation in plants.

Most of the identified Cd hyperaccumulators to date, including *T. caerulescens* and *A. halleri*, are also able to hyperaccumulate Zn, implying that similar mechanisms of Zn and Cd accumulation may exist in these plant species (Verbruggen et al., 2009). In the Cd hyperaccumulator *A. halleri*, the uptake and translocation of Zn and Cd in the plants may share the same pathway to a certain extent (Bert et al., 2002; Zhao et al., 2006; Ueno et al., 2008), and in vivo XRF mapping showed that Cd accumulation was positively correlated with that of Zn (Küpper et al., 2000; Hokura et al., 2006; Fukuda et al., 2008). The existence of interactions between Cd and Zn has also been suggested in the Cd hyperaccumulators *T. praecox* and *T. caerulescens* Ganges ecotype (Küpper et al., 2004; Ma et al., 2005; Pongrac et al., 2010). In this study, a positive association of Cd and Zn was observed in the nonaccumulator NHE *S. alfredii* (Fig. 1). However, in the leaves and stems of the HE *S. alfredii*, it was clearly shown that the distribution patterns of Cd and Zn were quite distinct (Figs. 2, 3, and 6), as Cd was largely localized in the parenchyma tissues, while Zn was predominantly localized to epidermal and vascular cells (Tian et al., 2009). This indicates that different storage mechanisms are probably involved in the hyperaccumulation of Cd and Zn by the Cd/Zn hyperaccumulator *S. alfredii*.

Cd shares many physical similarities (charge and ionic radius) with Ca. In plants, Cd may permeate through Ca channels from guard cells (Perfus-Barbeoch et al., 2002) and root cells (White, 2000). Recently, it has been reported that the Arabidopsis (*Arabidopsis thaliana*) protein *AtHMA1*, which functions as a Ca^{2+} pump, may help to concentrate Cd in organelles or mediate its extrusion to the extracellular medium (Moreno et al., 2008). In the HE *S. alfredii*, Cd uptake and translocation was previously shown to be positively associated with the Ca pathway (Lu et al., 2008, 2010), and when plants of the HE *S. alfredii* were exposed to a higher Ca-Cd ratio, an enhanced tolerance to Cd was observed (Lu et al., 2010; Tian et al., 2011). This study showed a close spatial association of Cd and Ca in HE *S. alfredii* plants, which, to our knowledge, has not previously been observed in any Cd hyperaccumulator. The distribution pattern of Cd was very different from that for Ca in the hyperaccumulators *A. halleri* (Küpper et al., 2000; Hokura et al., 2006; Fukuda et al., 2008) and *T. praecox* (Vogel-Mikus et al., 2008b). These results suggest that Cd accumulation and detoxification in HE *S. alfredii* plants may be associated with metal transport through Ca channels or transporters. This hypothesis contrasts with current models of Cd accumulation, which suggest that Cd accumulation may be governed by common genetic determinants with that of Zn accumulation in hyperaccumulators (Hanikenne et al., 2008; Verbruggen et al., 2009). This study suggests that interactions between Cd and Ca should be considered more closely in future physiological and molecular investigations of Cd hyperaccumulation in

Table III. *Concentrations of organic acids in roots, stems, and leaves of the HE S. alfredii under Cd exposure*

Plants were treated with 0 or 100 μM Cd for 30 d. The results are presented as means of three replications.

Sample	Cd Levels	Malic Acid	Citric Acid	Oxalic Acid
	μM		$\mu mol\ g^{-1}$ *fresh wt*	
Young leaves	0	35.9 ± 4.6	2.3 ± 0.1	1.2 ± 0.0
	100	43.6 ± 5.8	2.7 ± 0.2	1.3 ± 0.3
Mature leaves	0	38.9 ± 4.0	2.8 ± 0.3	1.0 ± 0.2
	100	46.0 ± 4.9	3.0 ± 0.5	1.1 ± 0.2
Stems	0	36.2 ± 4.8	2.3 ± 0.2	1.2 ± 0.2
	100	43.6 ± 5.3	2.7 ± 0.7	1.4 ± 0.4
Roots	0	6.1 ± 0.2	5.3 ± 1.2	2.8 ± 0.4
	100	7.2 ± 0.7	7.8 ± 1.1	3.8 ± 0.3

plants, although it is possible that this is a mechanism unique to the HE *S. alfredii*.

Vacuoles have been suggested to be the primary site of accumulation of a number of heavy metals, including Cd (Conn and Gilliham, 2010). This study showed that Cd in HE *S. alfredii* plants accumulated preferentially in the parenchyma tissues (pith, cortex, and mesophyll), all of which consist of large vacuolar cells, supporting the contention that vacuoles may serve as major storage sites for Cd in this plant species. This is also supported by fluorescence imaging of Cd in the leaves of the HE *S. alfredii* (Supplemental Fig. S2) using the Cd probe Leadmium Green AM dye (Lu et al., 2008).

The acidic environment of the vacuole provides a favorable environment for the formation of metal-organic acid complexes (Haydon and Cobbett, 2007). In *A. halleri*, the majority of Cd that was preferentially localized in the trichomes was found to be divalent and bound to O or nitrogen (N) ligands, not S ligands (Fukuda et al., 2008), although Cd translocated from roots to shoots was predominantly in inorganic forms (Ueno et al., 2008). In roots and shoots of *T. praecox*, up to 80% of the Cd ligands were O ligands that were provided by the cell walls and by organic acids stored in vacuoles (Vogel-Mikus et al., 2010). The results reported here for Cd speciation in the HE *S. alfredii*, based on x-ray absorption spectroscopy analysis, also suggest that the majority of the Cd in this ecotype is sequestered within the vacuoles in association with O ligands (Table I) and is dominantly similar to the Cd-malate complex (Table II). Kramer (2010) suggested that the capacity for organic acid accumulation in a plant might determine its maximum divalent cation accumulation. Determination of the organic acid component in the HE *S. alfredii* also showed that malate was the most abundant organic acid in the plants (Table III). All these results indicate that Cd was probably coordinated with malate in HE *S. alfredii* plants. The results obtained by Zhang et al. (2010) suggested that phytochelatin (PC) synthesis might act as the major intracellular Cd detoxification mechanism in shoots of the Cd hyperaccumulator *S. alfredii* as in nonresistant plants. This finding, however, was observed under a very high Cd level (500 μM), which might cause toxicity even for the hyperaccumulator *S. alfredii*. Furthermore, the association of Cd and PCs was detected after complex sample preparation (Zhang et al., 2010), whereas our experiments were conducted on frozen hydrated plant samples under very low temperature. From an energetic point of view, metals are also more likely to be stored in vacuoles weakly bound by organic acids, rather than investing energy for synthesizing the large amounts of strong ligands such as PCs for complexation (Küpper et al., 2004, 2009). Thus, these results suggest that Cd would be more likely to be associated with malate rather than PCs or GSH in the storage sites of the HE *S. alfredii* plants.

The malate concentration in the leaves and stems of the HE *S. alfredii*, however, was not increased significantly by increasing Cd concentration in the solution, suggesting that malate synthesis is not induced by Cd. This result is very similar to that previously reported for another Cd hyperaccumulator, *T. caerulescens* (Ueno et al., 2005). These results support the view that high organic acid concentrations in the hyperaccumulators may be a prerequisite for metal hyperaccumulation, rather than a specific response to metal hyperaccumulation or hypertolerance (Kramer, 2010). As suggested by Ueno et al. (2005), the complex forms of Cd-organic acids inside the vacuoles might be the result of an efficient tonoplast transport of Cd and a constitutively high concentration of malate in the vacuoles. Thus, the transporters involved in Cd efflux into the vacuoles, especially those related to Ca transport such as CAX members (Verbruggen et al., 2009), are of relevance for future research on the molecular mechanisms of the Cd hyperaccumulator *S. alfredii*.

MATERIALS AND METHODS

Plant Culture

Seedlings of two contrasting ecotypes of *Sedum alfredii* were cultivated hydroponically. Seeds of the HE of *S. alfredii* were obtained from an old Pb/Zn mine area in Zhejiang Province in China, and the NHE of *S. alfredii* was obtained from a tea plantation of Hangzhou in Zhejiang Province. The seeds of two *S. alfredii* ecotypes were germinated on a mixture of perlite and vermiculite moistened with deionized water. Four weeks after germination, the plants were subject to 4 d of exposure of one-fourth-, one-half-, and full-strength nutrient solution containing 2 mM Ca^{2+}, 4 mM NO_3^-, 1.6 mM K^+, 0.1 mM $H_2PO_4^-$, 0.5 mM Mg^{2+}, 1.2 mM SO_4^{2-}, 0.1 mM Cl^-, 10 μM H_3BO_3, 0.5 μM $MnSO_4$, 5 μM $ZnSO_4$, 0.2 μM $CuSO_4$, 0.01 μM $(NH_4)_6{\cdot}Mo_7O_{24}$, and 100 μM Fe-EDTA. Nutrient solution pH was adjusted daily to 5.8 with 0.1 N NaOH or HCl. Plants were grown in a growth chamber with a 16/8-h photoperiod at 400 μmol m^{-2} s^{-1}, day/night temperatures of 26°C/20°C, and day/night humidity of 70%/85%. The nutrient solution was continuously aerated and renewed every 4 d.

Seedlings of the two precultured ecotypes of *S. alfredii* were exposed to different treatments (0, 10, 100, and 400 μM Cd). Each treatment was replicated three times. Plants were harvested after Cd exposure for 30 d. The plants of NHE did not grow at high Cd treatments (100 and 400 μM) after 30 d.

Elemental Mapping for Stems and Leaves by μ-XRF and LA-ICP-MS

Analyses

Fresh stems and leaves were cut from plants after 30-d treatments and rinsed. The midtransverse areas of stem samples at similar developmental stages were selected from both ecotypes for comparison. Sections (100 μm thick) of samples were cut with a cryotome (Leica CM1950). Briefly, stem and leaf samples were frozen by liquid nitrogen and fixed immediately on specimen disks using deionized water at the actively cooled (−40°C) speciation quick-freezing shelf. After about 10 min, samples were subjected to sectioning at a temperature of −20°C, and sections in good condition were selected and freeze dried at −20°C for 3 d (Tian et al., 2010). μ-XRF imaging was performed on beamline 13-ID-C (GSECARS; proposal no. 23899) at the Advanced Photon Source. The incident x-ray beam was focused using a pair of Kirkpatrick-Baez mirrors, and the incident beam was monochromatized using a Si(111) double-crystal monochromator. μ-XRF maps were collected using either a Vortex single-element or four-element solid-state silicon detector (SII NanoTechnology) at room temperature. For μ-XRF mapping, the incident beam was set at 30 keV. During the experiments, the spot size of the x-ray beam was 2 × 2 μm^2, which is much smaller than the size of most leaf and stem cells in *Sedum*. μ-XRF maps were obtained by rastering the beam in 5-μm steps, with a count time of 0.1 s per step, for the following major and minor/

trace elements: P, S, chlorine (Cl), K, Ca, Mn, Fe, nickel, copper, Zn, rubidium, Pb, and Cd.

LA-ICP-MS Measurement

LA-ICP-MS measurements of element distribution in the plant samples of the HE *S. alfredii* treated with 100 μM Cd for 30 d were performed by the Interdisciplinary Center for Plasma Mass Spectrometry at the University of California at Davis using an Agilent 7500A ICP-MS apparatus (Agilent Technologies). Helium (0.85 L min^{-1}) was used as the transport gas from the New Wave laser ablation cell and was mixed with argon gas (1.05 L min^{-1}). The LA-ICP-MS system was tuned for sensitivity prior to each experiment using the National Institute of Standards and Technology (NIST) 612 glass standard. The formation of oxides was minimized by monitoring mass-to-charge ratio 248/232 ($^{232}Th^{16}O^+/^{232}Th^+$) values lower than 0.2% (Wu et al., 2009). The elemental maps of the samples were determined by LA-ICP-MS under the optimized experimental parameters summarized in Supplemental Table S1 at room temperature.

Standard preparation and quantification were performed according to Becker et al. (2008) and Wu et al. (2009) with modifications. SRM NIST 1570a spinach (*Spinacia oleracea*) leaves were used for the standard calibration of the analytical data. The spinach leaves were spiked with standard solutions of Cd from 0 to 5,000 mg L^{-1}. After absorption for 72 h, the materials, together with the stem and leaf samples of the HE *S. alfredii*, were dried at 75°C until constant weight was reached and then ground into fine powder. Standard reference materials SRM NIST 1515 apple (*Malus domestica*) leaves and SRM NIST 1515 peach (*Prunus persica*) leaves were used to validate the analytical procedure. One-half gram of each standard material and plant sample was weighed and pressed into a pellet without any binder under 8-atm pressure. The pelletized materials and plant samples were analyzed for elemental concentrations by LA-ICP-MS and then subjected to further digestion and element determination by ICP-MS according to Lu et al. (2008). Elemental concentrations in the plant samples of the HE *S alfredii* measured by LA-ICP-MS are similar to those analyzed by ICP-MS (Supplemental Table S2). The whole leaf and stem and leaf cross sections of the HE *S. alfredii* were analyzed using LA-ICP-MS. Stem and leaf cross sections were prepared similar to those subject to μ-XRF analysis. The ion intensities of $^{13}C^+$, $^{111}Cd^+$, $^{44}Ca^+$, $^{39}K^+$, $^{63}Cu^+$, $^{24}Mg^+$, $^{54}Mn^+$, $^{66}Zn^+$, $^{56}Fe^+$, $^{31}P^+$, and $^{34}S^+$ were recorded. $^{13}C^+$ was used as the internal standard to compensate for the water content effect and the possible inhomogeneity of the materials. The ratio of the $^{13}C^+$ ion intensity plotted against the concentration of the spike in the standard was used to develop the calibration curves, and the distribution profiles of the elements in the scanned samples were quantified using these curves. The analytical procedures were validated by standard reference material SRM NIST 1547 peach leaves and SRM NIST 1515 apple leaves.

Bulk EXAFS

EXAFS data of powdered tissues (roots, stems, and leaves) from HE *S. alfredii* treated with 100 μM Cd for 30 d were collected at the Stanford Synchrotron Radiation Lightsource with the storage ring SPEAR-3 operating at 3 GeV and with ring currents of 80 to 100 mA. Cd K-edge spectra were recorded on beamline 7-3 (proposal nos. 3186 and 3482) with the same equipment conditions described in our previous study (Tian et al., 2010). The monochromator energy of each spectrum was calibrated using Cd metal foil between the second and third ionization chambers; its absorption edge was calibrated to an edge of 26,711 eV, and Cd K_α fluorescence were recorded using a 30-element germanium detector (Canberra Industries) equipped with Soller slits and silver filters.

Fresh plant tissues were prepared using liquid nitrogen and measured at 10 K in a liquid helium flow cryostat to minimize the breakdown and mixing of cellular components and to reduce the loss of intensity in the signal (Tian et al., 2010). Spectra were collected for standard Cd species including $Cd(NO_3)_2$ (solution), Cd-malate, Cd-glutathione, Cd-Cys, Cd-His, Cd-oxalate, Cd-citrate, and Cd-cell wall. All solutions were prepared in 30% glycerol to prevent ice crystal formation. The complexes Cd-malate, Cd-Cys, Cd-His, Cd-oxalate, Cd-citrate, and Cd-glutathione were made by adding 5.0 mM citrate, Cys, His, oxalate, malate, or glutathione to an aqueous solution of 0.5 mM Cd $(NO_3)_2$ at pH 5.5. Root cell wall material was exposed to 0.5 mM $Cd(NO_3)_2$ in hydroponic solution (final pH of 6) for 72 h, rinsed in deionized water, and frozen in liquid nitrogen for storage. Spectra of all plant samples and standard solution samples were recorded in fluorescence mode, while spectra of solid standard samples were recorded in transmission mode. Detuning of the primary beam by 50% was performed to reject higher harmonic reflections.

EXAFS Data Analysis

Multiple scans (six to 12, depending on Cd concentration) were collected and averaged for each sample to improve the signal-to-noise ratio. The spectra data of each sample were calibrated to the Cd K-edge (26,711 eV) in the program SixPack (Webb, 2005). The normalization of the EXAFS spectra was carried out according to standard methods using the SixPack program suite. The spectra were normalized to unit step height using a linear preedge and postedge background subtraction and transformed to *k*-space based on E0 = 26,711 eV. The *k*-function was extracted from the raw data by subtracting the atomic background using a cubic spline consisting of 7 kn set at an equal distance fit to K^3-weighted data, and K^3-weighted (k) functions were Fourier transformed over the 1.5 to 12 $Å^{-1}$ range using a Kaiser-Bessel window with a smoothing parameter of 4. Fits were performed in the R-space on both real and imaginary parts of RSF contributions to obtain the identity of the back-scattering atoms, Cd-neighbor distance (R), coordination number (N), and the Debye-Waller factor (σ2) for each scattering path (Pokrovsky et al., 2008). Theoretical back-scattering amplitude and phase-shift functions for Cd-O, Cd-N, Cd-S, Cd-Cl, Cd-C, and Cd-Cd single and multiple scattering paths were computed using the FEFF8 ab initio code (Ankudinov et al., 1998). The K^3-weighted EXAFS spectra were also least-squares fitted over a wave vector (k) range of 1.5 to 12 $Å^{-1}$ using a combination of Cd compound standards. Best fits were derived by incrementally increasing the number of fit components and minimizing the fit residual. The range for the fit was varied as a function of data quality and in order to test contributions from minor components.

Organic Acid Assay

Organic acids in plant samples of the HE *S. alfredii* treated with or without 100 μM Cd were analyzed according to the methods described by Yang et al. (2006).

Statistical Analysis

All data were statistically analyzed using the SPSS package (version 11.0), ANOVA was performed on the data sets, and means and SE of each treatment of corresponding data were calculated.

Supplemental Data

The following materials are available in the online version of this article.

Supplemental Figure S1. Biomass and Cd concentrations of the HE and NHE *S. aflredii* after Cd treatments (0, 10, 100, and 400 μM) for 30 d.

Supplemental Figure S2. Visualization of Cd in leaf cross sections of the HE *S. alfredii* using the Cd fluorophore, Leadmium Green AM dye.

Supplemental Table S1. LA-ICP-MS operating conditions.

Supplemental Table S2. Comparison of the nutrient element concentrations in the plant samples of the HE *S. alfredii* measured by LA-ICP-MS (using standard reference material NIST SRM 1570a spinach leaves for calibration) and ICP-MS after digestion.

ACKNOWLEDGMENTS

We express our sincere gratitude to Dario Cantu and Naoaki Ikemiyagi of the University of California, Davis, and to all the staff of BL 7-3, BL 2-3, and BL 9-3 at the Stanford Synchrotron Radiation Lightsource, particularly Serena DeBeer, Samuel M. Webb, and Matthew Latimer, for their support. Portions of this research were carried out at the Stanford Synchrotron Radiation Lightsource, a Directorate of the Stanford Linear Accelerator Center National Accelerator Laboratory and an Office of Science User Facility operated by the U.S. Department of Energy Office (DOE) of Science by Stanford University. The Stanford Synchrotron Radiation Lightsource Structural Molecular Biology Program is supported by the DOE Office of Biological and Environmental Research and by the National Institutes of Health, National Center for Research

Resources, Biomedical Technology Program (grant no. P41RR001209). Use of the Advanced Photon Source, an Office of Science User Facility operated for the U.S. DOE of Science by Argonne National Laboratory, was supported by the U.S. DOE (contract no. DE-AC02-06CH11357).

Received July 22, 2011; accepted October 23, 2011; published October 24, 2011.

LITERATURE CITED

Alonso-Blanco C, Aarts MGM, Bentsink L, Keurentjes JJB, Reymond M, Vreugdenhil D, Koornneef M (2009) What has natural variation taught us about plant development, physiology, and adaptation? Plant Cell **21:** 1877–1896

Ankudinov AL, Ravel B, Rehr JJ, Conradson SD (1998) Real-space multiple-scattering calculation and interpretation of x-ray-absorption near-edge structure. Phys Rev B **58:** 7565–7576

Baker AJM, McGrath SP, Reeves RD, Smith JAC (2000) Metal hyperaccumulator plants: a review of the ecology and physiology of a biological resource for phytoremediation of metal-polluted soils. *In* N Terry, G Bañuelos, eds, Phytoremediation of Contaminated Soil and Water. Lewis Publishers, Boca Raton, FL, pp 85–107

Becker JS, Dietrich RC, Matusch A, Pozebon D, Dressier VL (2008) Quantitative images of metals in plant tissues measured by laser ablation inductively coupled plasma mass spectrometry. Spectrochim Acta B At Spectrosc **63:** 1248–1252

Bert V, Bonnin I, Saumitou-Laprade P, de Laguerie P, Petit D (2002) Do Arabidopsis halleri from nonmetallicolous populations accumulate zinc and cadmium more effectively than those from metallicolous populations? New Phytol **155:** 47–57

Chaney RL, Angle JS, Broadhurst CL, Peters CA, Tappero RV, Sparks DL (2007) Improved understanding of hyperaccumulation yields commercial phytoextraction and phytomining technologies. J Environ Qual **36:** 1429–1443

Conn S, Gilliham M (2010) Comparative physiology of elemental distributions in plants. Ann Bot (Lond) **105:** 1081–1102

Cosio C, DeSantis L, Frey B, Diallo S, Keller C (2005) Distribution of cadmium in leaves of Thlaspi caerulescens. J Exp Bot **56:** 765–775

Deng DM, Shu WS, Zhang J, Zou HL, Lin Z, Ye ZH, Wong MH (2007) Zinc and cadmium accumulation and tolerance in populations of Sedum alfredii. Environ Pollut **147:** 381–386

Fukuda N, Hokura A, Kitajima N, Terada Y, Saito H, Abe T, Nakai I (2008) Micro x-ray fluorescence imaging and micro x-ray absorption spectroscopy of cadmium hyper-accumulating plant, *Arabidopsis halleri* ssp *gemmifera*, using high-energy synchrotron radiation. J Anal At Spectrom **23:** 1068–1075

Hall JL (2002) Cellular mechanisms for heavy metal detoxification and tolerance. J Exp Bot **53:** 1–11

Hanikenne M, Talke IN, Haydon MJ, Lanz C, Nolte A, Motte P, Kroymann J, Weigel D, Krämer U (2008) Evolution of metal hyperaccumulation required cis-regulatory changes and triplication of HMA4. Nature **453:** 391–395

Haydon MJ, Cobbett CS (2007) Transporters of ligands for essential metal ions in plants. New Phytol **174:** 499–506

Hokura A, Onuma R, Kitajima N, Terada Y, Saito H, Abe T, Yoshida S, Nakai I (2006) 2-D x-ray fluorescence imaging of cadmium hyperaccumulating plants by using high-energy synchrotron radiation x-ray microbeam. Chem Lett **35:** 1246–1247

Hu ZC, Liu YS, Gao S, Hu SH, Dietiker R, Gunther D (2008) A local aerosol extraction strategy for the determination of the aerosol composition in laser ablation inductively coupled plasma mass spectrometry. J Anal At Spectrom **23:** 1192–1203

Kramer U (2010) Metal hyperaccumulation in plants. Annu Rev Plant Biol **61:** 517–534

Küpper H, Götz B, Mijovilovich A, Küpper FC, Meyer-Klaucke W (2009) Complexation and toxicity of copper in higher plants. I. Characterization of copper accumulation, speciation, and toxicity in *Crassula helmsii* as a new copper accumulator. Plant Physiol **151:** 702–714

Küpper H, Lombi E, Zhao FJ, McGrath SP (2000) Cellular compartmentation of cadmium and zinc in relation to other elements in the hyperaccumulator *Arabidopsis halleri*. Planta **212:** 75–84

Küpper H, Lombi E, Zhao FJ, Wieshammer G, McGrath SP (2001) Cellular compartmentation of nickel in the hyperaccumulators *Alyssum lesbiacum, Alyssum bertolonii* and *Thlaspi goesingense*. J Exp Bot **52:** 2291–2300

Küpper H, Mijovilovich A, Meyer-Klaucke W, Kroneck PMH (2004) Tissue- and age-dependent differences in the complexation of cadmium and zinc in the cadmium/zinc hyperaccumulator *Thlaspi caerulescens* (Ganges ecotype) revealed by x-ray absorption spectroscopy. Plant Physiol **134:** 748–757

Lu LL, Tian SK, Yang XE, Wang XC, Brown P, Li TQ, He ZL (2008) Enhanced root-to-shoot translocation of cadmium in the hyperaccumulating ecotype of *Sedum alfredii*. J Exp Bot **59:** 3203–3213

Lu LL, Tian SK, Zhang M, Zhang J, Yang XE, Jiang H (2010) The role of Ca pathway in Cd uptake and translocation by the hyperaccumulator *Sedum alfredii*. J Hazard Mater **183:** 22–28

Ma JF, Ueno D, Zhao FJ, McGrath SP (2005) Subcellular localisation of Cd and Zn in the leaves of a Cd-hyperaccumulating ecotype of *Thlaspi caerulescens*. Planta **220:** 731–736

Moreno I, Norambuena L, Maturana D, Toro M, Vergara C, Orellana A, Zurita-Silva A, Ordenes VR (2008) AtHMA1 is a thapsigargin-sensitive Ca^{2+}/heavy metal pump. J Biol Chem **283:** 9633–9641

Pence NS, Larsen PB, Ebbs SD, Letham DLD, Lasat MM, Garvin DF, Eide D, Kochian LV (2000) The molecular physiology of heavy metal transport in the Zn/Cd hyperaccumulator Thlaspi caerulescens. Proc Natl Acad Sci USA **97:** 4956–4960

Perfus-Barbeoch L, Leonhardt N, Vavasseur A, Forestier C (2002) Heavy metal toxicity: cadmium permeates through calcium channels and disturbs the plant water status. Plant J **32:** 539–548

Pokrovsky OS, Pokrovski GS, Feurtet-Mazel A (2008) A structural study of cadmium interaction with aquatic microorganisms. Environ Sci Technol **42:** 5527–5533

Pongrac P, Vogel-Mikus K, Vavpetic P, Tratnik J, Regvar M, Simcic J, Grlj N, Pelicon P (2010) Cd induced redistribution of elements within leaves of the Cd/Zn hyperaccumulator *Thlaspi praecox* as revealed by micro-PIXE. Nucl Instrum Methods Phys Res B **268:** 2205–2210

Punshon T, Guerinot ML, Lanzirotti A (2009) Using synchrotron x-ray fluorescence microprobes in the study of metal homeostasis in plants. Ann Bot (Lond) **103:** 665–672

Robinson BH, Lombi E, Zhao FJ, McGrath SP (2003) Uptake and distribution of nickel and other metals in the hyperaccumulator *Berkheya coddii*. New Phytol **158:** 279–285

Sun YB, Zhou QX, An J, Liu WT, Liu R (2009) Chelator-enhanced phytoextraction of heavy metals from contaminated soil irrigated by industrial wastewater with the hyperaccumulator plant (Sedum alfredii Hance). Geoderma **150:** 106–112

Tian SK, Lu LL, Yang XE, Labavitch JM, Huang YY, Brown P (2009) Stem and leaf sequestration of zinc at the cellular level in the hyperaccumulator *Sedum alfredii*. New Phytol **182:** 116–126

Tian SK, Lu LL, Yang XE, Webb SM, Du YH, Brown PH (2010) Spatial imaging and speciation of lead in the accumulator plant Sedum alfredii by microscopically focused synchrotron x-ray investigation. Environ Sci Technol **44:** 5920–5926

Tian SK, Lu LL, Zhang J, Wang K, Brown PH, He ZL, Liang J, Yang XE (2011) Calcium protects roots of Sedum alfredii H. against cadmium-induced oxidative stress. Chemosphere **84:** 63–69

Ueno D, Iwashita T, Zhao FJ, Ma JF (2008) Characterization of Cd translocation and identification of the Cd form in xylem sap of the Cd-hyperaccumulator Arabidopsis halleri. Plant Cell Physiol **49:** 540–548

Ueno D, Ma JF, Iwashita T, Zhao FJ, McGrath SP (2005) Identification of the form of Cd in the leaves of a superior Cd-accumulating ecotype of Thlaspi caerulescens using ^{113}Cd-NMR. Planta **221:** 928–936

Verbruggen N, Hermans C, Schat H (2009) Molecular mechanisms of metal hyperaccumulation in plants. New Phytol **181:** 759–776

Vogel-Mikus K, Arcon I, Kodre A (2010) Complexation of cadmium in seeds and vegetative tissues of the cadmium hyperaccumulator *Thlaspi praecox* as studied by x-ray absorption spectroscopy. Plant Soil **331:** 439–451

Vogel-Mikus K, Regvar M, Mesjasz-Przybyłowicz J, Przybyłowicz WJ, Simcic J, Pelicon P, Budnar M (2008a) Spatial distribution of cadmium in leaves of metal hyperaccumulating *Thlaspi praecox* using micro-PIXE. New Phytol **179:** 712–721

Vogel-Mikus K, Simcic J, Pelicon P, Budnar M, Kump P, Necemer M, Mesjasz-Przybyłowicz J, Przybyłowicz WJ, Regvar M (2008b) Comparison of essential and non-essential element distribution in leaves of the Cd/Zn hyperaccumulator *Thlaspi praecox* as revealed by micro-PIXE. Plant Cell Environ **31:** 1484–1496

Webb SM (2005) SIXpack: a graphical user interface for XAS analysis using IFEFFIT. Phys Scr **115:** 1011–1014

White PJ (2000) Calcium channels in higher plants. Biochim Biophys Acta **1465:** 171–189

Wu B, Zoriy M, Chen Y, Becker JS (2009) Imaging of nutrient elements in the leaves of *Elsholtzia splendens* by laser ablation inductively coupled plasma mass spectrometry (LA-ICP-MS). Talanta **78:** 132–137

Wu QT, Wei ZB, Ouyang Y (2007) Phytoextraction of metal-contaminated soil by Sedum alfredii H: effects of chelator and co-planting. Water Air Soil Pollut **180:** 131–139

Yang XE, Li TQ, Yang JC, He ZH, Lu LL, Meng FH (2006) Zinc compartmentation in root, transport into xylem, and absorption into leaf cells in the hyperaccumulating species of *Sedum alfredii* Hance. Planta **224:** 185–195

Yang XE, Long XX, Ni WZ, Fu CX (2002) *Sedum alfredii* H: a new Zn hyperaccumulating plant first found in China. Chin Sci Bull **47:** 1634–1637

Yang XE, Long XX, Ye HB, He ZL, Calvert DV, Stoffella PJ (2004) Cadmium tolerance and hyperaccumulation in a new Zn-hyperaccumulating plant species (*Sedum alfredii* Hance). Plant Soil **259:** 181–189

Zhang ZC, Chen BX, Qiu BS (2010) Phytochelatin synthesis plays a similar role in shoots of the cadmium hyperaccumulator *Sedum alfredii* as in non-resistant plants. Plant Cell Environ **33:** 1248–1255

Zhao FJ, Jiang RF, Dunham SJ, McGrath SP (2006) Cadmium uptake, translocation and tolerance in the hyperaccumulator Arabidopsis halleri. New Phytol **172:** 646–654

Zhao FJ, Lombi E, Breedon T, McGrath SP (2000) Zinc hyperaccumulation and cellular distribution in *Arabidopsis halleri*. Plant Cell Environ **23:** 507–514

Zhao FJ, McGrath SP (2009) Biofortification and phytoremediation. Curr Opin Plant Biol **12:** 373–380